International Journal of Electrical, Electronic and Communication Sciences
ISSN: 2517-9438
Vol:4, No:11, 2010

Quantitative quality assessment of microscopic image mosaicing

Alessandro Bevilacqua[1,2], Alessandro Gherardi[2], Filippo Piccinini[2]

Abstract—**The mosaicing technique has been employed in more and more application fields, from entertainment to scientific ones. In the latter case, often the final evaluation is still left to human beings, that assess visually the quality of the mosaic. Many times, a lack of objective measurements in microscopic mosaicing may prevent the mosaic from being used as a starting image for further analysis.**

In this work we analyze three different metrics and indexes, in the domain of signal analysis, image analysis and visual quality, to measure the quality of different aspects of the mosaicing procedure, such as registration errors and visual quality. As the case study we consider the mosaicing algorithm we developed. The experiments have been carried out by considering mosaics with very different features: histological samples, that are made of detailed and contrasted images, and live stem cells, that show a very low contrast and low detail levels.

Index Terms—**mosaicing, quality assessment, microscopy, stem cells**

I. Introduction

IMAGE mosaicing is a well known technique used to wide the (microscope) field of view by collecting and stitching together overlapping images of the same scene. The outcome, the mosaic, may undergo several effects from as many causes: uneven lighting condition of the image field of view, registration errors to compute the transformation between images, stitching and, finally, moving objects that mislead the feature matching algorithm. Nevertheless, the most traditional way to evaluate the quality of microscopic image mosaics is still based on visual evaluation of experts, or simply, end users. For instance, the authors in [1] conceive a complex mosaicing algorithm for automated microscopes and limited overlapping area between images. The results, referring to histological samples and cells, just report visual considerations regarding evidences of misalignment and stitching. Or else, the mosaics achieved in [2] with an automated microscope have been visually compared with the frozen histology. A few other works try introducing the concept of objective assessment. This concept in [3] refers to mosaics of urban scenes and concerns the interest points matching and the radiometric correction processes. Besides visual evaluation, a reconstruction error is built as the mean of the intensity difference between two successive images on the overlapping area. In [4], the authors build synthetic virtual slides to be used as the ground truth about the positioning accuracy of a stitching algorithm for virtual microscopy. Besides testing visually the algorithm on several real world examples, the authors compute the positioning error mean μ and standard deviation σ of the Euclidean distance between the supposed and the computed translational vector.

The reason why this happens is due to the mosaics usually not being used for measuring purposes. On the contrary, we aim to apply to the mosaic the algorithm we have already developed for segmentation of skin cells [5] and to devise proper segmentation algorithms to characterize stem cells. In this paper, we consider three well known metrics and indexes to give measures of visible defects arising from stitching effects, uneven illumination of the microscope field of view, geometric misalignments. These measurements regard generic signal analysis (Mean Square Error, MRE), image signal analysis (Peak Signal-to-Noise Ratio, PSNR) and visual analysis (Universal Quality Index, UQI). This work is organized as follows. Sect. II outlines the image mosaicing stages while Sect. III gives details of their most significant sources of error. Sect. IV describes the metrics and the indexes we use to give measures regarding the quality of microscopic image mosaics. Two mosaics built of histological and stem cell images are analyzed in Sect. V and their quality measured according to the numerical and the visual point of view. Some conclusions are drawn in Sect. VI and some proposal for future works are given.

II. Mosaicing: an outline

Image mosaicing in the field of microscopy can be performed in different ways, depending whether the microscope has an automated stage holder or not. Modern automated microscopes are usually endowed with the option of performing image mosaicing by using known translations of the motorized stage. Through this expensive option, the mosaic is composed by stitching the images according to the known relative positions. Otherwise, the stage holder is positioned manually: in this case, the mosaic can be built by using image registration techniques and exploiting a suitable overlap between the images of the captured sequence. In any case, the problem is twofold: aligning images from a geometric point of view and achieving a seamless stitching even in the presence of abrupt changes in lighting conditions within an image. The former can be solved by a geometric registration, whereas the latter requires a tonal registration. In order to better understand the errors that affect the system, we first outline the mosaicing method we adopted.

A. Registration

The registration model can be set to different kinds of transformation: translative, affine and projective one, according to the design of the image acquisition system and the geometry of the object being imaged. In case of microscopy, due to

[1] DEIS (Department of Electronics, Computer Science and Systems), University of Bologna; alessandro.bevilacqua@unibo.it
URL:http://cvg.deis.unibo.it
[2] ARCES (Advanced Research Centre on Electronic Systems), University of Bologna; {abevilacqua, agherardi, fpiccinini}@arces.unibo.it

the geometry of the system, the mapping between points on two consecutive images can be reasonably achieved through a translative model. However, in a real world scenario, yet more in case of manual movements, the ideal translational motion of the stage is only a simplification, since the camera principal axis of the optical system might not be perfectly normal to the holder's plane. Moreover, there can be a misalignment also between the components of the stage such that a drift along the two moving directions might occur.

To the purpose of this work, we can assume the effects of such misalignment as being negligible, and we choose a pure translative model. Images are aligned by detecting and matching features in a common overlapping region by tracking features extracted in two consecutive acquired frames, using a frame-to-frame (F2F) registration strategy. We have chosen the Kanade-Lucas-Tomasi feature tracker (KLT) [6][7] since it can achieve a high accuracy and its computational cost is compatible with a real-time application of the method. A fast initial guess, based on a phase-correlation approach [8], is computed to guide the KLT tracker in case of large displacements of the holder position. The phase correlation guess is used as a coarse estimation of the holder displacements, this granting additional benefits in terms of robustness and performance. Once the tracker has found enough reference points in the common region, the transformation matrix H is estimated according to the given model by using a robust estimator to eliminate outliers (RANSAC, [9]) and solving the overdetermined equation system.

B. Image warping

The registration procedure is able to calculate the transformation matrix at a sub-pixel level. Accordingly, the image warping is based on interpolation techniques. Here, we have chosen not to use any blending mask in order to evaluate the quality of our registration method right along the stitching regions. Images are warped into the mosaic frame through a bi-linear interpolation by overwriting all the transformed pixels belonging to each image. Depending on our choice, images are also tonally aligned by using our method described in [10][11].

III. Types of errors

In order to assess the quality of the resulting mosaic, different sources of error have to be considered. Firstly, there can be errors due to the *registration* algorithm, which are purely geometric errors, due to the least square nature of the fitting of the estimated transformation matrix, although the outliers have been removed by RANSAC. Secondly, since we are dealing with discrete image grids, the procedures of image *warping and stitching* in the common mosaic's reference frame may affect the quality of the mosaic, depending on the chosen interpolation method. Moreover, we can have errors due to the differences in reflected light captured in subsequent images, due to *varying lighting conditions*. This results in a tonally misaligned mosaic, where the vignetting effect prevents a seamless stitching along the overlapping regions. Lastly, *moving objects* due to residue of cells or biological matter in the medium may alter the image content in the shared region of two subsequent images. In this case, with a blending operation the mosaic would even undergo ghosting effects.

Table I resumes the contribution of the main errors.

Table I
The main errors that affect the mosaic quality.

Error	description
geometric	registration error due to feature tracking and model fitting
interpolation	warping interpolation error due to discrete images
tonal	tonal misalignment of consecutive frames
content	fast moving objects (residue) may alter image content

All these errors contribute to the final quality of the generated mosaic.

IV. Error metrics

Given a Region Of Interest (ROI) R, let $R_I(x,y)$ and $R_M(x,y)$ be the pixel values of this ROI in (x,y) in the original image and in the corresponding part of the mosaic, accordingly. In order to quantify the quality of final mosaic, we have evaluated the following error metrics and indexes:

- Mean Square Error (MSE)

$$MSE = \frac{\sum_x \sum_y (R_I(x,y) - R_M(x,y))^2}{N} \quad (1)$$

- Peak Signal to Noise Ratio (PSNR)

$$\text{PSNR} = 10 log_{10} \frac{N \cdot (max(R_M) - min(R_M))^2}{\sum_x \sum_y (R_I(x,y) - R_M(x,y))^2} \quad (2)$$

- Universal Quality Index (UQI) as defined in [12].

Also, by registering again the first image at the end of the sequence, we can analyze the pure geometrical error. In fact, an error-free registration would give a matrix concatenation equal to the identity matrix. However, geometric errors will show non null offsets of δx and δy in the translative model matrix:

$$T = \prod_{i=1}^{n} H_i = \begin{bmatrix} 1 & 0 & \delta x \\ 0 & 1 & \delta y \\ 0 & 0 & 1 \end{bmatrix}$$

where n is the total number of images in the sequence. As for the pure geometric registration error we have used the ℓ_2 norm of these offsets.

V. Experimental results

Two sequences (H9 and C9) of eight different images taken from histological samples (I) and Mesenchimal Stem Cells (M), respectively, have been used to build closed path mosaics. Also, these mosaics have been built with (T) and without (NT) tonal registration, this accounting altogether for four evaluated mosaics. In all the generated mosaics, for measurement purposes the first image is added again at the end of the registration, therefore the length of the sequences becomes of 9 images. Accordingly, we need to perform one more registration than needed and expected. In this way, we manage to evaluate the pure geometric registration error: since the first image used as a reference has never been altered, the last and the first image must coincide.

Table II shows the error analysis using metrics and indexes described in Sect. III, while Table III contains the registration error. Let start by considering the sequence with histological samples. Its high detail level permits the reader to better detect the visual quality. Figure 1 shows the mosaic generated by the

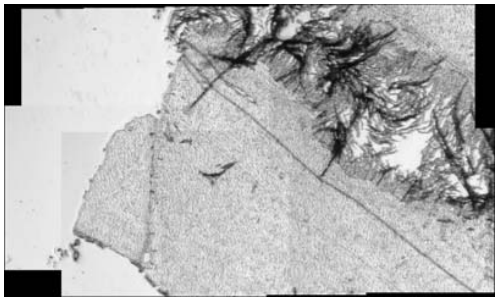

Fig. 1. Mosaic for the sequence H9 NT, without tonal registration.

sequence H9 without using our tonal registration algorithm. Several reasons may yield a different illumination field over the same sample region when it is positioned in different parts of the microscope's field of view. As one can see, stitching artifacts are clearly visible. In Figure 2, the mosaic

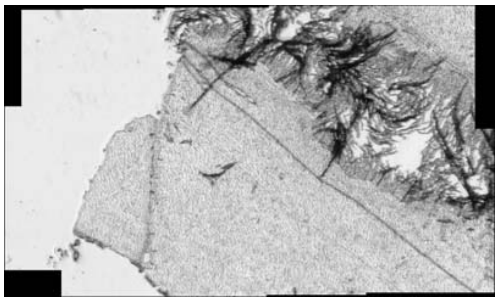

Fig. 2. Mosaic for the sequence H9 T, with tonal registration.

generated by the same histological sequence H9 is shown, now with images preprocessed by our tonal alignment algorithm. Stitching artifacts have now been disappeared. As one can see, the quality index UQI increases while both the errors decrease.

Table II
QUALITY METRICS AND INDEXES.

	MSE	PSNR	UQI
H9 NT	136.11	26.32	0.976
H9 T	71.36	29.32	0.986
C9 NT	12.52	33.59	0.820
C9 T	7.52	35.80	0.871

As for the stem cells sequence, these images have very a low contrast that is yet more evident in the printed copy. This yields values of MSE lower than in the histological samples. The lack of reference points makes the visual evaluation more difficult, thus yielding lower UQI's. Figure 3(a) shows the mosaic generated by the sequence C9 without using our tonal registration algorithm. In Figure 3(b), the benefit of our

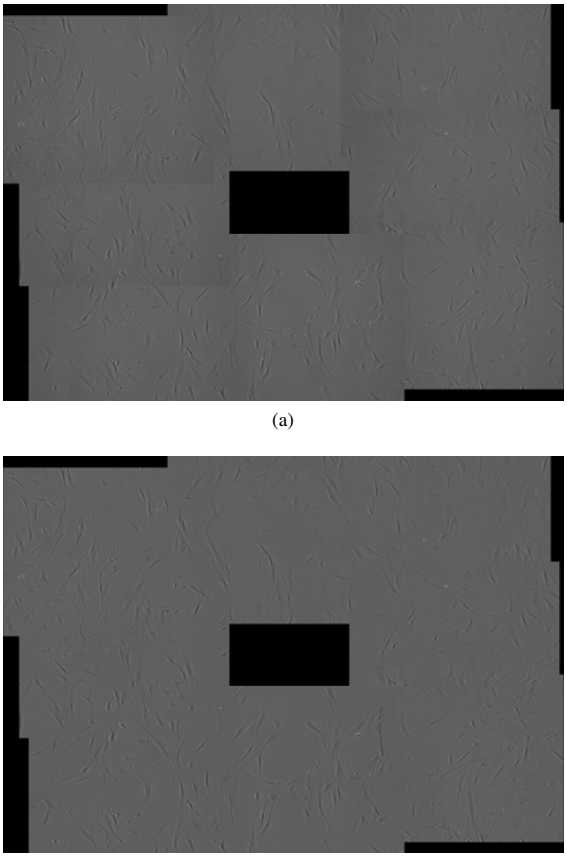

(a)

(b)

Fig. 3. Mosaic built with sequence C9, without tonal registration (a) and with our tonal registration method (b).

tonal registration method is quite evident. Again, the values of Table II shows the same behavior than the previously examined couple of mosaics. The lack of details also make the registration process harder. In fact, the stronger the reference points or structures present in the images, the more reliable the match found by the registration algorithm. In fact, Table III confirms that the registration error increase of about 10% with respect to the histological samples. In general, these metrics and indexes permit to *quantify* the diverse improvement introduced in the mosaic algorithm. Accordingly, we can notice that in percentage the best improvement carried out by our tonal registration is for UQI with stem cells ($\tilde{7}\%$), while it is for PSNR ($\tilde{1}1\%$) and MSE ($\approx 48\%$) with the histological section.

As a concluding remark as far as our mosaicing algorithm is concerned, we can state that all the mosaics present better values when generated by using our tonal alignment method and that our registration algorithm always yields geometric error keeping below half a pixel, this resulting in a very good geometric alignment.

VI. CONCLUSIONS

This work analyzes the effectiveness of three well known metrics and indexes to measure the quality of microscopic image mosaics. Using our mosaicing algorithm as a case

Table III
GEOMETRIC ERRORS.

	Geometric error (pixel)
H9	0.31
C9	0.43

study, we come to prove and *quantify* some general statements. Images with a higher gradient magnitude and a better defined contrast, like the histological ones, show a high UQI while permitting a better sub-pixel alignment than low-contrast images, like those depicting stem-cells. Nevertheless, a lower misalignment error can yield higher errors and a lower peak SNR.

We are now working towards the definition of indexes and metrics that are as much independent as possible from the pixel values. In this way, besides achieving reliable differential measures of mosaics of the same scene build using different methods, these metrics will become a standardize method for measuring quality of images with different global photometric features.

ACKNOWLEDGMENTS

We would like to thank the biologist Dr. Enrico Lucarelli and his staff of the Bone Regeneration Laboratory (BRL) of the Rizzoli Orthopedic Institute (Bologna, Italy) for providing the data used in this work.

REFERENCES

[1] C. Sun, R. Beare, V. Hilsenstein, and P. Jackway, "Mosaicing of microscope images with global geometric and radiometric corrections," *Journal of Microscopy*, vol. 224, no. 2, pp. 158–165, Nov. 2006.
[2] D. Gareau, Y. Patel, Y. Li, I. Aranda, A. Halpern, K. Nehal, and M. Rajadhyaksha, "Confocal mosaicing microscopy in skin excisions: a demonstration of rapid surgical pathology," *Journal of Microscopy*, vol. 233, no. 1, pp. 149–159, Jan. 2009.
[3] E. Zagrouba, W. Barhoumi, and S. Amri, "An efficient image-mosaicing method based on multifeature matching," *Machine Vision and Applications*, vol. 20, pp. 139–162, 2009.
[4] D. Steckhan, T. Bergen, T. Wittenberg, and S. Rupp, "Efficient large scale image stitching for virtual microscopy," in 30^{th} *Annual International IEEE EMBS Conference Vancouver, British Columbia, Canada, August 20-24*, Aug. 2008, pp. 4019–4023.
[5] A. Bevilacqua, A. Gherardi, and M. Ferri, "Predicting biological age from a skin surface capacitive analysis," *Int. J. Mod. Phys. C*, vol. 15, no. 9, pp. 1309–1320, 2004.
[6] B. D. Lucas and T. Kanade, "An iterative image registration technique with an application to stereo vision," in *International Joint Conference on Artificial Intelligence*, 1981, pp. 674–679.
[7] J. Y. Bouguet, "Pyramidal implementation of the Lukas Kanade feature tracker: Description of the algorithm," *In Intel Research Laboratory, Technical Report*, pp. 1–9, 1999.
[8] H. Foroosh, J. B. Zerubia, and M. Berthod, "Extension of phase correlation to subpixel registration," *IEEE Transactions on Image Processing*, vol. 14, no. 1, pp. 12–22, 2002.
[9] M. A. Fischler and R. C. Bolles, "Random sample and consensus: A paradigm for model fitting with application to image analysis and automated cartography," *Comm. of the ACM*, vol. 24, no. 6, pp. 381–395, 1981.
[10] A. Bevilacqua, A. Gherardi, L. Carozza, and F. Piccinini, "Semi-automatic background detection in microscopic images," in *International Conference on Biological Science and Engineering (ICBSE), Venice, Italy, November 24-26*, 2010.
[11] P. Azzari and A. Bevilacqua, "Joint spatial and tonal mosaic alignment for motion detection with ptz camera," *Lecture Notes in Computer Science*, vol. 4142, pp. 764–775, 2006.
[12] Z. Wang and A. C. Bovik, "A universal image quality index," *IEEE Signal Processing Letters*, vol. 9, no. 3, pp. 81–84, Mar. 2002.